

## THE EVOLUTION OF RESEARCH AND DEVELOPMENT ON COCHLEAR BIOMODEL

### Article history

Received

12 June 2015

Received in revised form

19 September 2015

Accepted

5 December 2015

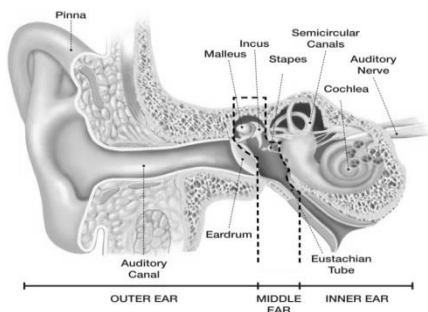
Thailis Bounya Ngelayang<sup>a\*</sup>, Low Yin Fen<sup>a</sup>, Rhonira Latif<sup>b</sup>,  
Burhanuddin Yeop Majlis<sup>b</sup>

<sup>a</sup>Faculty of Electronics and Computer Engineering (FKEKK), Universiti Teknikal Malaysia Melaka, Hang Tuah Jaya, 76100 Durian Tunggal, Melaka, Malaysia

<sup>b</sup>Institute of Microengineering and Nanoelectronics (IMEN), Universiti Kebangsaan Malaysia, 43600 UKM, Bangi, Selangor, Malaysia

\*Corresponding author  
thai\_isz@yahoo.com

### Graphical abstract



### Abstract

The research and development of the cochlear biomodels have initially started over a century ago. Since then, various types of approach have been implemented in trials to perfectly replicate the nature of the human auditory system. The evolution started with the implementation of mechanical elements into the cochlear biomodel operating in air and fluidic surrounding. However, due to the huge size of the mechanical cochlear biomodel, the microelectromechanical systems (MEMS) has been implemented in order to attain a life-sized cochlear biomodel. Researchers have looked into the possibilities of fabricating the MEMS cochlear biomodel in air and fluidic mediums. In this paper, the mechanical and MEMS cochlear biomodel implementations will be reviewed. The key part in modelling the cochlea for human auditory system is to mimic closely its nature and capabilities in terms of the geometrical design, material properties and sensory performance.

Keywords: Artificial Basilar Membrane, Cochlear Biomodel, Human Auditory System, Microelectromechanical Systems (MEMS)

© 2016 Penerbit UTM Press. All rights reserved

## 1.0 INTRODUCTION

Ever since Helmholtz proposed the resonance theory of hearing in 1863, many researches in cochlear biomodelling have been conducted in order to obtain better understanding on the nature of human auditory system [1]. Immense efforts have been attempted by researchers to replicate every single component that built up the auditory system. Above all components, basilar membrane is the most important part in auditory system that transduces the incoming sound wave into mechanical vibration and electrical nerve impulses. The adaptive mechanism in the basilar membrane allows the level of the perceived sound to be sensed and controlled.

In the basilar membrane, different segments along the membrane with thousands of small hair cells structure behave as a series of tuned resonators. These partitions allow the sensing of high frequency tones, specifically towards the base segment of the membrane which is the opening part of the basilar membrane.

Meanwhile, the low frequency tones are sensed by partitions towards the apex segment located at the end of the basilar membrane. In response to a single incoming tone, only a certain region of the membrane which corresponds to the frequency of the incoming tone will vibrate. This insinuates the tonotopic organization or place-to-frequency mapping characteristics of the membrane. Thus, the

basilar membrane possesses the ability to encode and break down the incoming sound wave into its frequency components. In normal human cochlear, the lowest sound frequency of 20 Hz can be detected and the highest is up to 20 kHz [2].

In this paper, the human auditory hearing mechanism is discussed and the performances of the developed two different types of cochlear biomodels to mimic the human auditory hearing mechanism are reviewed. The implementation of mechanical and microelectromechanical systems (MEMS) into the cochlear biomodel that operates in both air and fluidic surroundings will be analysed accordingly.

## 2.0 HUMAN AUDITORY SYSTEM

Figure 1 shows the cross sectional diagram of a human auditory system. It consists of three different parts, namely the outer ear, the middle ear and the inner ear. The outer ear consists of a pinna, an auditory canal and an ear drum that directs and carries the sound waves from surrounding into a narrow tube leading to the middle ear. At the end of the auditory canal, these sound waves bump into a thin membrane known as the eardrum. The middle ear consists of the smallest bones in human body known as the ear bones. The ear bones are made up of three miniature bones called the malleus, incus and stapes. Malleus is connected to the eardrum and its movement is triggered by the eardrum vibration. This movement subsequently leads to the movement of incus and stapes.

In the inner ear, the stapes is connected to the cochlea which is a liquid-filled coiled chamber containing basilar membrane and hair cells that detects the incoming movement from the middle ear. The thickness, width and stiffness of the basilar membrane vary along the length of the cochlea and vibrates due to the motions exerted by the ear bones [3, 4]. The basilar membrane within the cochlea filters the mechanical movement into different frequency bands and the hair cells converts the mechanical movements into nerve impulses that eventually will be transmitted to the brain.

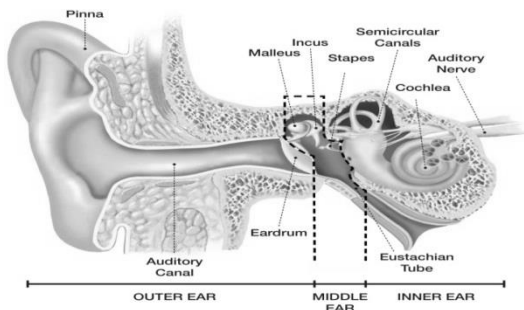


**Figure 1** The cross sectional diagram of a human auditory system

## 3.0 MECHANICAL IMPLEMENTATION

The implementation of mechanical element into the cochlear biomodel has the ability to mimic naturally the auditory signal processing function of the basilar membrane. These mechanical cochlear biomodels have been developed either in air or fluidic surrounding. The development of a mechanical cochlear biomodel has been reported to focus on the material properties and geometrical dimensions of the mechanical membranes / resonators. Initially, the geometrical size for the developed mechanical cochlear biomodel is huge as compared to the real cochlea. Due to its large size, the measured output level of the perceived sound can be extremely high. Only then the scaling technique is adopted to make the size to be comparable.

### 3.1 Mechanical Implementation in Air Surrounding

In 2004, Chan Keen Leong has reported to develop two mechanical cochlear biomodels with single and double chambers. The chambers have been built using Perspex blocks with dimensions of 130 mm length, 55 mm width and 45 mm height as shown in Figure 2. A silicon rubber of 1.0 mm thickness has been employed in the chamber to represent the basilar membrane. Each chamber has one cylindrical slot which has been positioned to face the same end and thus, represents the oval and round windows of the cochlea. The frequency selectivity from both cochlear biomodels has been compared.

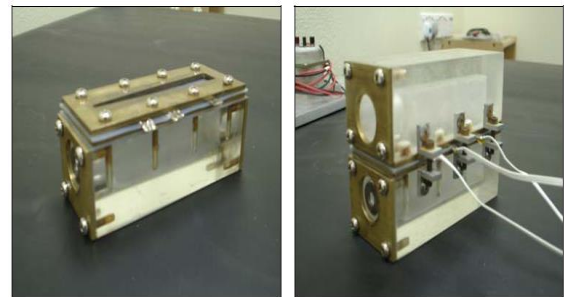


**Figure 2** The single chamber model (left) and the double chamber model (right) reported to be Chan Keen Leong cochlear biomodels

Strain measurements have been conducted on both single chamber model and double chamber model. An accelerometer was attached to the shaker to mimic the travelling input sound waves applied on the stapes of the cochlea. Dynamic signal analyzer supplied the sine waves from 20 Hz to 2 kHz at 1 Vrms to the shaker.

The points on the tapered slot were measured using laser interferometer and strain gauges. The single chamber model was introduced first to determine the conversion factor between the laser and the strain-frequency response measurements

from the silicon rubber membrane. Double chamber model was then tested and the dependent frequency of the conversion factor from the relating laser has been yielded.

Figure 3 shows the frequency response of the single chamber model and the double chamber model. The strain in volt has been normalized with respect to the shaker input. The tested positions on the membrane were taken at 25 mm and 80 mm from the narrow end of the tapered slot. The measurement result in Figure 3 (a) shows that the resonant frequency was recorded to be 300 Hz at position 25 mm and 150 Hz at position 80 mm for the single chamber model. For double chamber model in Figure 3 (b), the resonant frequency was found to be 10 times larger. Chan Keen Leong has reported that the presence of the standing waves in the single chamber model has caused the high frequency energy to propagate along the cochlear duct and thus, the strain gauges cannot measure the strain adequately [5,6].

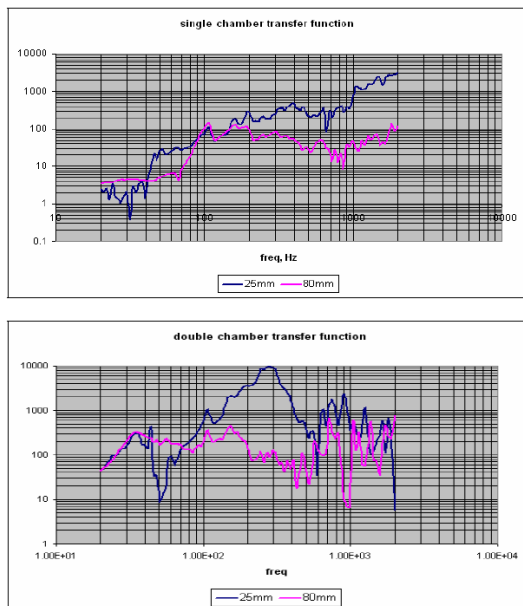


**Figure 3** The frequency transfer function on the single chamber and double chamber model

The nonlinear velocity-based feedback control law was applied to a cochlear biomodel designed by Bryan S Joyce and Pablo A Tarazaga in 2014. Their proposed cochlear biomodel mimic the nonlinear cochlear amplification [7].

The cochlear biomodel consists of aluminium cantilever beams with piezoelectric actuators as shown in Figure 4. The cantilever beams have the dimensions of 47.0 cm x 3.80 cm x 0.30 cm with four Mide' QuickPack™ piezoelectric actuators. The two actuators located at the tip of the beams were used to supply disturbance excitation,  $d(t)$ . Another two actuators at the root of the beams were used to

control vibration based on the control signal,  $u(t)$ . The nonlinear velocity-based feedback control law helps to reduce the linear viscous damping of the cantilever beam.

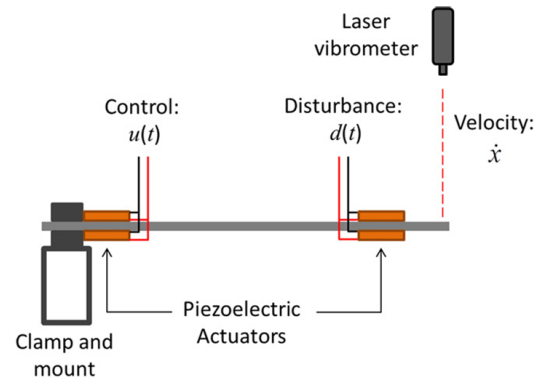


**Figure 4** The cochlear biomodel proposed by Bryan S Joyce and Pablo A Tarazaga which uses cantilever beams with four Mide' QuickPack™ piezoelectric actuators that set up the disturbance excitation,  $d(t)$  and control vibration based on the control signal,  $u(t)$

The close loop system was created through the feedback control law. This system has the capability to undergo a supercritical Hopf bifurcation where the system function is to obtain equilibrium. Once the system reaches its equilibrium point, the magnitude of the system response is subjected to the forcing amplitude frequency. Any increment in the magnitude response will also increase the equivalent damping [8, 9, 10]. This represents the concept of increment in sound pressure when it enters human cochlear.

Polytech PDV 100 laser Doppler vibrometer was used to measure the tip velocity of the beams and dSPACE system was used to control and acquire the measured data. Figure 5 shows the simulated and measured velocity and gain of the system near the first natural frequency with variation of excitation levels. When there is no control being implemented, the system is linear and has the same gain at every frequency regardless of the input amplitude. However, when the control signal is in place, the tip velocity shows a compressive nonlinearity at their first natural frequency.

Similar to the natural cochlear behavior, the amplification in this designated system affects a small band of frequencies at the first natural frequency and the bandwidth of the resonant peak increases with the increase of excitation amplitudes.

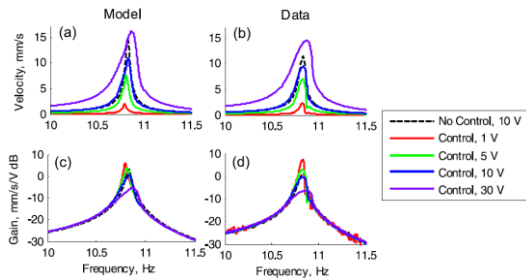


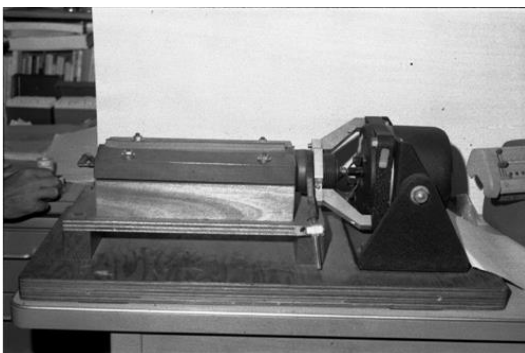
**Figure 5** The simulated (a) velocity and (c) gain from the Simulink model at different excitation levels. The measured (b) velocity and (d) gain using laser vibrometer

### 3.2 Mechanical Implementation in Fluidic Surrounding

In 1961, Georg Von Békésy was awarded with a noble prize for his revision on resonance theory in human auditory system. He observed the cochlear partition motion in a human cadaver. The observation was based on the travelling waves that were initiated by the incoming sound waves and propagated along the basilar membrane.

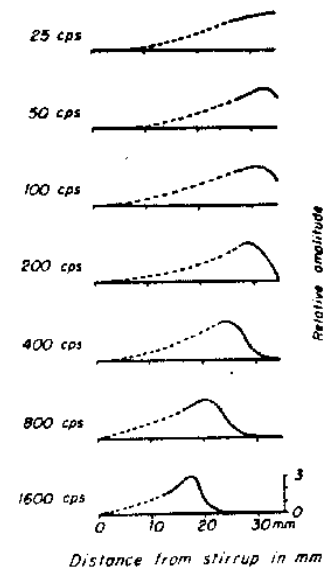
Georg firstly has carried out one nondestructive dissection on a human cochlear. During the dissection process, a special grinding mechanism has been performed in a water bath. The travelling waves were observed from the stroboscopic examination of the silver particles motion that has been sprinkled on the dissected basilar membrane. The observation concludes that the travelling waves achieved the maximum amplitude at different locations along the basilar membrane, depending on the applied frequency of the incoming sound waves [11].

Once the dissection process was completed, Georg built up a mechanical model of the inner ear. This model consists of a plastic tube filled with water. The model has a membrane of 30 cm length. Figure 6 shows the mechanical model of the inner ear with one large vibrator connected to the right side to produce frequency controlled stimulus.



**Figure 6** The mechanical cochlear biomodel designed by Georg. A large vibrator is connected to the right side of the model to produce frequency controlled stimulus

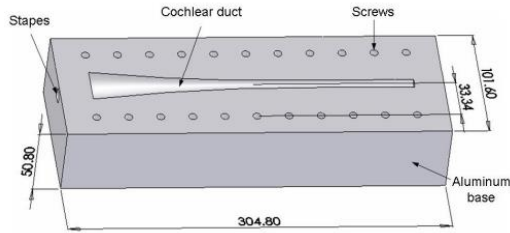
From the developed mechanical cochlear biomodel, it was observed that the travelling waves propagated along the whole length of the membrane at approximately constant amplitude. However, at one certain spot, the amplitude was reported to have a maximum magnitude. Figure 7 shows the displacement measurement of the basilar membrane as a function of position along the membrane's length at input frequencies applied from 25 cps to 1600 cps. When the stimulus frequency increases, the sensed vibration section travels towards the piston that represents the stapes which is located near the apex of the basilar membrane [12]. On the other hand, when the stimulus frequency decreases, the section area of the sensed vibration moves in the opposite direction towards the base of the basilar membrane.



**Figure 7** The measurement of basilar membrane displacement as a function of position along the length of the membrane at different input frequency

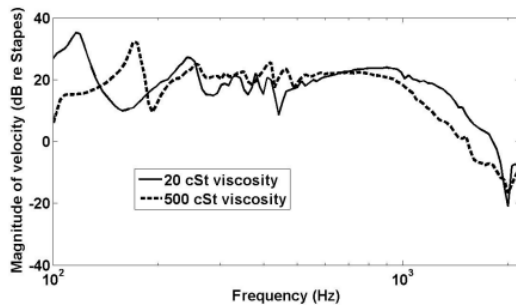
An investigation on hydromechanical cochlear biomodel of the Gerbil cochlear was conducted by Shuangqin Liu and his team in 2008. This model investigates the natural frequency of the Gerbil cochlear that has been scaled up to 16 times of its real size. The model was built with only one cochlear duct with the dimension of 304.80 mm length, 101.60 mm width and 50.80 mm height.

Figure 8 shows the design of the cochlear duct and its base. Polyoxymethylene membrane is used to represent the basilar membrane. In this study, the width size of the basilar membrane is varied. The cochlear duct is built with aluminium base and filled with silicon oil at two different viscosities of 20 cSt and 500 cSt.



**Figure 8** The dimension of the cochlear duct and its base made by Shuangjin Liu et al

The input to the cochlear biomodel is driven by a shaker at different frequency. The movement of the basilar membrane was measured with laser vibrometer at different points along the membrane's length. The sinusoidal signal with a range of 100 Hz to 20000 Hz was applied to the shaker to stimulate the basilar membrane at each measuring point.



**Figure 9** The influence of 20cSt and 500 cSt silicon oil viscosity on the measured velocity of the basilar membrane

Figure 9 shows the comparison of the measured velocity from the basilar membrane at two different viscosity of the silicon oil. For this two particular silicon oil, the experiment shows that in the developed cochlear biomodel, the viscosity of oil did not demonstrate significant influence to the membrane vibration. The natural frequency corresponds to the maximum displacement at one particular point on the basilar membrane [13, 14, 15]. At 2 cm from base, the natural frequency response is measured to be 7000 Hz while at point of 15 cm from base, the natural frequency is 350 Hz.

#### 4.0 MICROELECTROMECHANICAL SYSTEM (MEMS) IMPLEMENTATION

Microelectromechanical system (MEMS) consists of miniaturise mechanical and electrical elements that operates at the microscopic level. Due to the large size and bulky effects of the mechanical cochlear implementation, MEMS has started to capture researchers interest in developing the life-sized cochlear biomodel. The MEMS resonator can act as

an electromechanical transducer that is able to perform the passive parallel spectral filtering and thus mimics the behavior of a basilar membrane. Via electrostatic effect, the MEMS resonator also possesses the capability to self-tune its sensitivity. MEMS cochlear biomodels have been reported to be developed either in air surrounding or in fluidic environment.

#### 4.1 Microelectromechanical System Implementation in Air Surrounding

With the rapid evolvement of the micromachining technology, various types of MEMS cochlear biomodels were developed and reported. Haronian and Macdonald proposed a microelectromechanics based artificial cochlear (MEMBAC) in 1995. In this model, an array of resonator beams with various lengths was etched together on a silicon substrate to function as an artificial basilar membrane. Figure 10 shows an electron micrograph image of the fabricated basilar membrane. Each resonator beam has a dimension of 1  $\mu\text{m}$  wide and 10  $\mu\text{m}$  thickness. The beam length varies from 400  $\mu\text{m}$  to 7000  $\mu\text{m}$ . 20  $\mu\text{m}$  gap was set in between the adjacent beams.

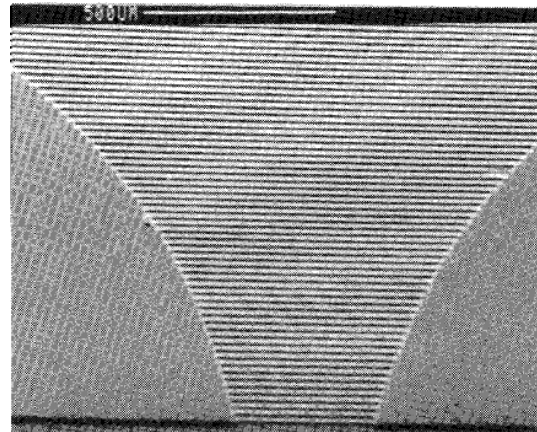


**Figure 10** MEMBAC model with resonator beam length varying from 400  $\mu\text{m}$  to 7000  $\mu\text{m}$

The developed MEMBAC consists of active and passive mechanical elements. The active part is represented by the Discrete Basilar Membrane (DBM) that consists of an array of acoustically coupled resonators and the electrical units that transfer signals from DBM to the information analyzing processor. The passive part is represented by the medium that surrounds DBM and the envelope structure that channels the acoustic signals to DBM. The envelope structure represents the outer and the middle ear [16].

MEMBAC has been tested in air at atmospheric pressure. Laser vibrometer was used to measure the natural frequency of the resonator beams. Figure 11 shows the sensitivity of several beams measured from

the fabricated MEMBAC as a function of frequency. All resonator beams have the same stiffness. The mass of each resonator beam is manipulated in order to change the natural frequency. Subsequently, this will also change the area between the adjacent resonators and will result in the change of damping. In this work, the natural frequency of the resonator beam changes from 20 kHz to 100 Hz as the beam mass increases [17].

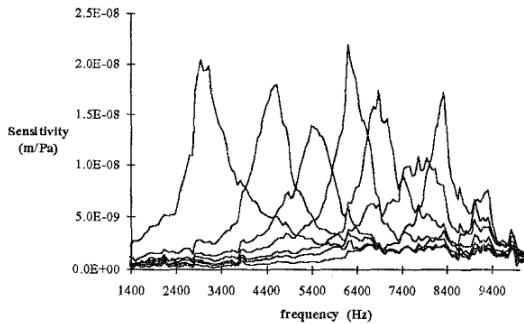


**Figure 11** Resonator beams sensitivity measurement from MEMBAC

The cochlear biomodel with fishbone structure was introduced by Kenji Tanaka and his team in 1997. For this structure, different lengths of silicon beams are fabricated on a backbone of a core material. Figure 12 shows the fishbone structure with transverse beam at the center supported by a diaphragm. This structure has thickness of 7  $\mu\text{m}$  with 62.5  $\mu\text{m}$  of resonator beam width and 205.5  $\mu\text{m}$  of resonator beam pitch.

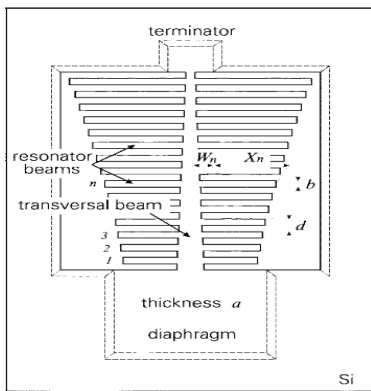


**Figure 12** Both sides of the transverse beam in the fishbone structure are supported by a diaphragm

The design concept of the fishbone structure consists of four desired criteria; 1) the structure is made of a flat board with constant thickness and Young's modulus. 2) The natural frequencies are linearly ordered in logarithmic scale. 3) The spacing distance between each resonator structure is equal.

4) The width and thickness dimensions of every resonator are equal [18, 19].

The flat-plate-type distributed resonators were implemented in the fishbone structure to equivalently replicate the fluid-mechanical action that occurs in the cochlea. Figure 13 shows the frequency response of the fishbone structure when all of the resonator beams are being stimulated to vibrate simultaneously. The result shows the tonotopic organization behavior of the basilar membrane. The amplitude variation from one resonator beam to another is reported to be due to the variation of the resonator beam area.

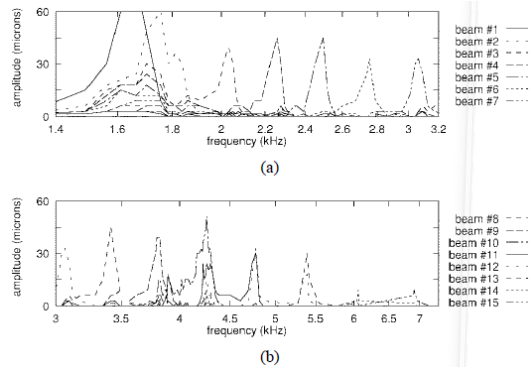


**Figure 13** The frequency response of the resonator beams after being stimulated to vibrate at the same time

The implementation of resonant gate transistor (RGT) in cochlear biomodel was introduced by Rhonira and her team in 2010. The proposed model consists of an array of RGT devices that possess the ability to self-adjust the sensitivity and frequency selectivity of the resonator bridges. Figure 14 shows the RGT device with an array of aluminium resonator mimicking the basilar membrane. The aluminium bridges vary in length from 0.278 mm to 1.618 mm to replicate the tonotopic organization behavior of the basilar membrane. The incoming acoustic signals are sensed by the aluminium bridges and then transformed into electrical signals that can be measured from the drain of RGT [20].

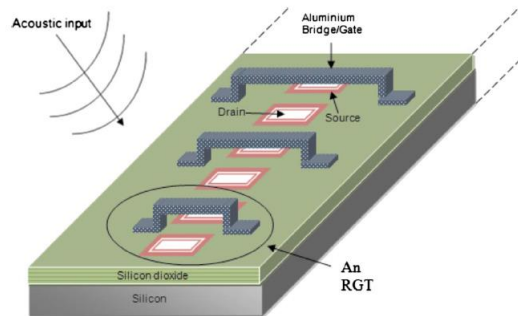


**Figure 14** An array of RGT devices that represent the basilar membrane of human cochlear

The aluminium bridges have been mechanically actuated using a piezoelectric disk. The laser vibrometer was used to measure the vibration amplitude and natural frequency of the aluminium bridges. The RGT devices have been designed to have natural frequencies from 1 kHz to 33.86 kHz. In Figure 15, the natural frequency for an aluminium bridge with length of 0.278 mm, 9  $\mu\text{m}$  wide and 0.5  $\mu\text{m}$  thick is presented. The measured natural frequency for that particular bridge is higher than the theoretical value which is 91 kHz. The difference between the measured and theoretical values has been suggested to be due to the residual stress remaining in the bridge structure [21].

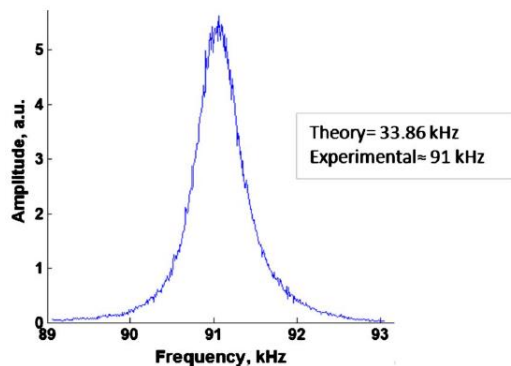


**Figure 15** The natural frequency measurement of an aluminium bridge with dimension of 0.278 mm long, 9  $\mu\text{m}$  wide and 0.5  $\mu\text{m}$  thick is 91 kHz which is higher than the theoretical calculated resonant frequency of 33.86 kHz

In 2013, Harto Tanujaya and his team have developed an artificial basilar membrane prototype using piezoelectric membrane made of polyvinylidene fluoride (PVDF) as shown in Figure 16. The PVDF membrane was bonded on a trapezoidal shape stainless steel plate with 30 mm length and 2 mm to 4 mm of width range. The thickness of the basilar membrane prototype is 40  $\mu\text{m}$ . 24 detecting electrodes were fabricated on top of the PVDF membrane using 500 nm aluminium thin film layer. The membrane and perforated trapezoid are mounted on a substrate channel with the dimensions of 47 cm x 17 cm and depth of 4 mm [22].

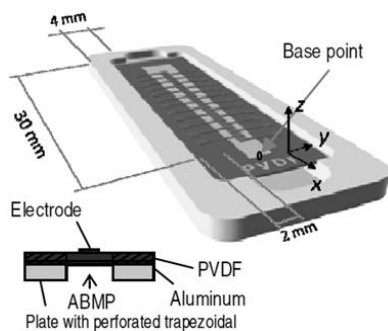


**Figure 16** The artificial basilar membrane design as reported by Harto Tanujaya

The experiment was carried out in atmospheric condition whereby the vibration of the membrane was measured from the electrode. The frequency selectivity characteristic of the basilar membrane has been studied. Figure 17 shows the contour map of the vibrating amplitude of the artificial basilar membrane prototype at 6 kHz, 9 kHz and 12.8 kHz. Maximum vibration amplitudes are observed at 25 mm for 6 kHz, 19 mm for 9 kHz and 9 mm for 12.8 kHz. The measurement results mimic the tonotopic organization characteristics of the basilar membrane as the acoustic waves travels from base to apex of the biological cochlear [23].

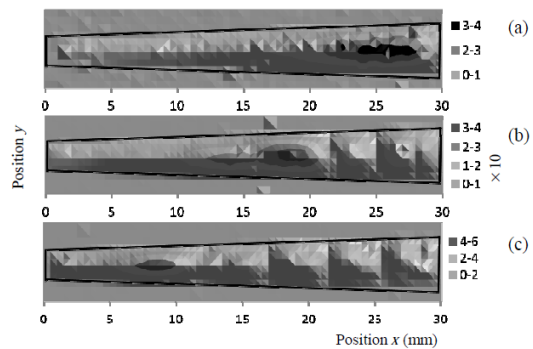


**Figure 17** Contour map of the vibrating amplitude of the artificial basilar membrane prototype at a) 6 kHz, b) 9 kHz, and c) 12.8 kHz

#### 4.2 Microelectromechanical System Implementation in Fluidic Surrounding

In 2002, Robert D. White and Karl Grosh studied the fluid structure travelling wave filters based on mammalian cochlear as shown in Figure 18. In their MEMS cochlear biomodel, the parallel beams array structure was developed with beam length in the range of 10  $\mu\text{m}$  to 20  $\mu\text{m}$ . The beams were separated with gaps in the range of 2  $\mu\text{m}$  to 4  $\mu\text{m}$ . The parallel beams array was fabricated by etching a silicon wafer, producing a silicon membrane structure. The two duct system was used and separated by the silicon membrane structure. The fluid duct has the dimension of 6.25 mm wide and 0.5 mm height. The silicon oil was employed as the fluid to be filled into the duct. Silicon oil was chosen as it is inert, safe and available in a wide range of viscosities.

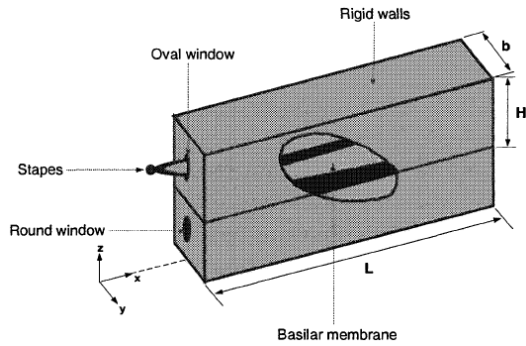


**Figure 18** The designed two ducts model by Robert D. White and Karl Grosh

Laser Doppler Velocimetry (LDV) was used to measure the displacement magnitude of the artificial basilar membrane. At 12 kHz to 62 kHz input, the measured displacements are in the range of 0.2 nm/Pa to 0.5 nm/Pa as presented in Figure 19. The maximum amplitude of the silicon membrane structure moved from base to apex of the MEMS cochlear biomodel [24, 25].

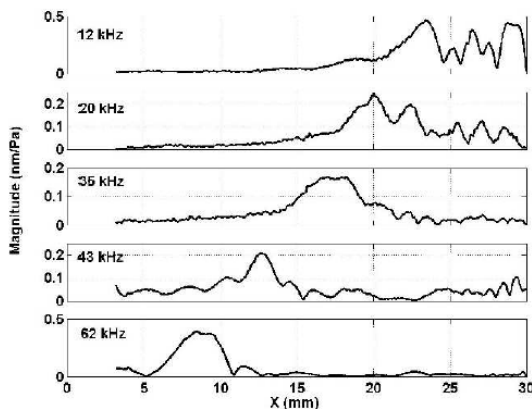


**Figure 19** Data from Laser Doppler Velocimetry (LDV) showing the magnitude of the membrane displacement. The basilar membrane response at magnitude 0.2 nm/Pa to 0.5 nm/Pa and frequency range in between 12 kHz to 62 kHz

Fangyi Chen and his team developed a hydromechanical biomimetic cochlear in 2006. Their model demonstrates the mimicking of three important cochlear features which are the travelling waves, the sharp high frequency rolloffs and the frequency selectivity. This model replicates the mechanical signal processing feature of a passive cochlea. In Fangyi model, the constructed artificial basilar membrane consists of a membrane substrate, beams and a frame to support it. 32 copper beams array were employed with length in the range of 4 mm to 8 mm. Piezofilm was used to build the membrane substrate that serves as a mechanical transducer in this model. A single fluid channel was employed on one side of the artificial basilar

membrane. The fluid channel structure was made from Plexiglas and then the structure was immersed in water [26]. Figure 20 shows the dimension of Fangyi's artificial basilar membrane.

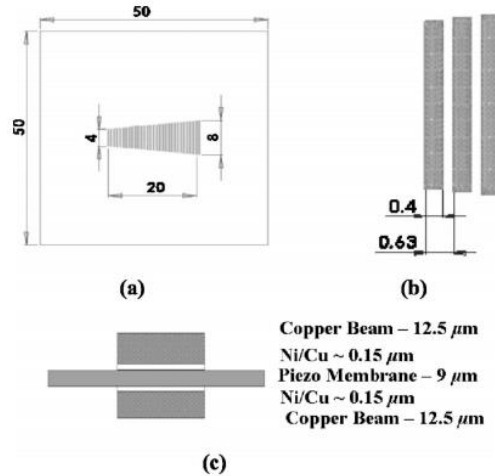


**Figure 20** The artificial basilar membrane with 32 beams. (a) The schematic layout showing the copper beams are arrayed on the substrate. (b) The zoom-in view of the beam structure. (c) A cross sectional view of a beam section where 9 μm piezo membrane is located in between 12.5 μm copper beams on both sides

The vibration of the beams on the membrane substrate was measured using laser scanning along the length of the beam. Piezomembrane voltage outputs were also measured with respect to the impulse stimulation [27]. The length of the beam is increased from beam #1 towards beam #32. The recorded sensitivity spectrum has shown that the impulse is small and narrow for beam #1 and becoming larger and wider towards beam #32. Figure 21 (a) represents the magnitude of sensitivity response for beam #32. The beam is highly sensitive at lower frequency. Figure 21 (b) shows the two distinct times when beam #32 oscillates the strongest. From this result, it is shown that high frequency input stimulation influences the resonance of shorter beams while low frequency stimulation influences the resonance of the longer beams on the developed basilar membrane.

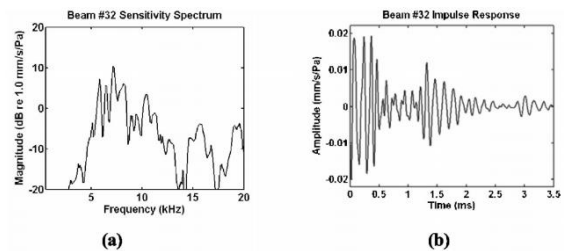


**Figure 21** The sensitivity response of beam #32 (a) in frequency domain and (b) in time domain

Hannes et al. in 2010 have reported to develop the derivation of fluid motion inside the cochlear duct by applying the conformal mapping method. Conformal mapping is analytically and numerically simple if being compared with other methods where the finite differences and image did not require approximations. The cochlear duct was designed with two dimensional half open boxes. The motions of cochlear fluid will create forces that will act on the cochlear partition. Damped oscillators were used to replicate the fluid motion inside the cochlear biomodel in order to recreate the forces that act on the cochlear partitions [28, 29].

In this mathematical analysis of the MEMS cochlear biomodel, 300 cochlear partition elements were designed with length of 33.5 mm and width of 0.2 mm. The duct height was set to 10 mm while the density of the cochlear fluid was taken to be  $10^{-3}$  kg/m<sup>3</sup>.

The cochlear biomodel was excited by pure tones from 20 Hz to 10240 Hz. The simulation result in Figure 22 shows an approximate logarithmic dependence of maximal amplitude upon the cochlear partition segment. The amplitude of the cochlear partition displacement depends on the partition that corresponds to the incoming frequencies.

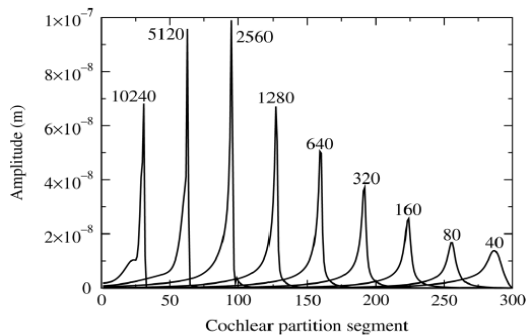


**Figure 22** The amplitude displacement response in a particular cochlear partition

## 5.0 CONCLUSION

Various types of cochlear biomodel implementations have been developed. This includes the consideration of the natural surrounding medium for the cochlear biomodel; either mechanically resonates in air or in fluidic environment. The early mechanical implementation possesses one obvious disadvantage as the physical size can be too huge as compared to the real cochlear. Subsequently, the displacement magnitude can be extremely high. In addition, for the cochlear biomodel that was implemented in fluidic surrounding, the developed model is passive and bulky. The latest micro-electromechanical system implementation is seen to have a bright future in cochlear biomodel development. First, the size of the developed MEMS

cochlear biomodel is in micrometer range and secondly the electronic circuitry can be incorporated into the model, especially in air surrounding medium. The focus on MEMS technology might be the right direction to follow for continuing the evolution of research and development of the cochlear biomodel. There are still lots of room for improvement in future in order to perfectly mimic the nature of a human cochlear.

## Acknowledgement

The authors would like to acknowledge Universiti Teknikal Malaysia Melaka for funding this project via the university Short Term Research Grant (PJP/2013/FKEKK(8B)/S01163) and the Ministry of Science, Technology and Innovation (MOSTI) for the ScienceFund grant (03-01-14 SF0095 L00023)

## References

- [1] Alexander Ellis, Helmholtz, and Hermann von. 1863. *On the Sensations of Tone as a Physiological basis of the Theory of Music*. New York: Dover Publications.
- [2] Dallos, P. 1996. *Overview: Cochlear Neurobiology in The Cochlea*. New York: Springer-Verlag.
- [3] Kaskel, A., Hummer, P. J., and Daniel, L. 1999. *Biology: An Everyday Experience*. New York: Glencoe/McGraw-Hill.
- [4] Lyshevski, S. E. 2007. *Mems And Nems: Systems, Devices And Structures*. Boca Raton: CRC press.
- [5] Chan Keen Leong. 2004. *Biomimetic Sensor Based On The Cochlea*. Singapore: National University of Singapore.
- [6] Bowen and Kwabena Boahen. 2003. *A Linear Cochlea Model With Bi-Directional Coupling*. USA: University of Pennsylvania.
- [7] Bryan, S. Joyce and Pablo, A. Tarazaga. 2014. Mimicking The Cochlear Amplifier in a Cantilever Beam Using Nonlinear Velocity Feedback Control. *Smart Material and Structures*. 23: 075019.
- [8] Martignoli, S., Van Der Vyver J. J., Kern, A., Cwate, Y. and Stoop, R. 2007. Analog Electronic Cochlea With Mammalian Hearing Characteristics. *Applied Physics Letter*. 9: 095018.
- [9] Camaler, S., Duke, T., Julicher, F. and Jacques, P. 2000. Auditory Sensitivity Provided by Self-Tuned Critical Oscillation of Hair Cells. *Proc. Natl. Acad. Sci. USA*. 97: 3183-8.
- [10] Egufluz, V. M., Ospeck, M., Choe, Y., Hudspeth, A. J. and Magnasco, M. O. 2000. Essential Nonlinearities in Hearing. *Physics Review Letter*. 84: 5232-5.
- [11] Békésy, von G. 1960. *Experiments in Hearing*. New York: McGraw Hill.
- [12] H. D. C. R. S. Elizabeth S. Olson. 2012. Von Békésy and cochlear mechanics, *Good Vibrations. A Special Issue To Honor The 50 Year Jubilee For Georg Von Békésy'S Nobel Prize The Physical Mechanisms Of Stimulation Within The Cochlea*. 293: 31-43.
- [13] Shuangqin, Liu, Douglas, A. Gauthier, Ethan Mandelup and Robert, D. White. 2008. Experimental Investigation of a Hydro-mechanical Scale Model of The Gerbil Cochlea. *ASME 2008 International Mechanical Engineering Congress and Exposition. Boston, USA*. 67778.
- [14] Duke, T. and Julicher, F. 2003. Active Travelling Waves in The Cochlea. *Physical Review Letters*. 90(15): 158101-1.

- [15] Zerlin, S. 1969. Travelling-wave Velocity in the Human Cochlea. *Journal of the Acoustic Society of America*. 46(4): 1011-15.
- [16] D. Haronian and N. C. MacDonald. 1995. A Microelectromechanics Based Artificial Cochlea (MEMBAC). *Proc. Int. Solid-State Sensors Actuators Conf.* 2: 0-3.
- [17] D. Haronian, and N. C. MacDonald. 1996. A Micromechanics-Based Frequency-Signature Sensor. *Sens. Actuators, A*. 53: 288-298.
- [18] K. Tanaka, M. Abe, and S. Ando. 1998. A Novel Mechanical Cochlea 'Fishbone' With Dual Sensor/Actuator Characteristics. *IEEE/ASME Trans. Mechatronics*. 3(2): 98-105.
- [19] M. Abe, S. Ando, K. Tanaka. 1997. Fishbone Architecture: An Equivalent Mechanical Model of Cochlea and Its Application to Sensors and Actuators. *Int. Conf. Solid-state Sensors Actuators*. Chicago. 1027-1030.
- [20] R. Latif, E. Mastropaolo, A. Bunting, T. J. Koickal, M. Newton, A. Hamilton, L. Smith, and R. Cheung. 2010. Microelectromechanical systems (MEMS) for biomimetic applications. *54th Int. Conf. Electron, Ion and Photon Beam Technology and Nanofabrication*. Anchorage. 28(6).
- [21] R. Latif. 2012. *Microelectromechanical Systems for Biomimetic Application*. Scotland: University of Edinburgh.
- [22] H. Tanujaya, H. Shintaku, and D. Kitagawa. 2013. Experimental and Analytical Study Approach of Artificial Basilar Membrane Prototype (ABMP). *Journal Engineering Technology Science*. 45(1): 61-72.
- [23] M. Wittbrodt, S. Puria and C. R. Steele. 2006. Developing a Physical Model of The Human Cochlea Using Micro-Fabrication Methods. *Audiology and Neurotology*. 11(2): 104-112.
- [24] R. D. White and K. Grosh. 2005. Design And Characterization Of MEMS Piezoresistive Cochlear-Like Acoustic Sensor. *ASME International Mechanical Engineering Congress And Exposition*. New Orleans, LA Acad. Sci. U.S.A. 102: 1296-1301.
- [25] R. D. White and K. Grosh. 2002. A Micromachined Cochlear-Like Acoustic Sensor. *Proceedings of SPIE, Smart Structures and Materials 2002: Smart Electronics, MEMS, and Nanotechnology*. 4700: 89-100.
- [26] Fangyi Chen, Howard I. Cohen, Thomas G. Bifano, Jason Castle, Jeffrey Fortin, Christopher Kapusta, Davis C. Mountain, Aleks Zosuls and Allyn E. Hubbard. 2006. A Hydromechanical Biomimetic Cochlea: Experiments and Models. *Journal of the Acoustic Society of America*. 119(1): 394-405.
- [27] T. P. Lechner. 1993. A Hydromechanical Model Of The Cochlea With Nonlinear Feedback Using PVF2 Bending Transducer. *Hear. Res.* 66: 202-212.
- [28] Hannes Luling, Jan Moritz P. Franosch and J. Leo van Hemmen. 2010. A Two-Dimensional Cochlear fluid Model Based On Conformal Mapping. *Journal of the Acoustic Society of America*. 128(6): 3577-3584.
- [29] O. F. Ranke. 1950. Theory of Operation of the Cochlea: A Contribution to the Hydrodynamics of the Cochlea. *Journal of the Acoustic Society of America*. 22: 772-777.